Salt Bridge in the Conserved His-Asp Cluster in *Gloeobacter* Rhodopsin Contributes to Trimer Formation

Takashi Tsukamoto,[†] Takashi Kikukawa,[†] Takuro Kurata,[†] Kwang-Hwan Jung,[‡] Naoki Kamo,[†] and Makoto Demura [†,*]

[†] Faculty of Advanced Life Science, Hokkaido University, Sapporo 060-0810, Japan

[‡] Department of Life Science and Institute of Biological Interfaces, Sogang University, Seoul 121-742, Republic of Korea

* Address correspondence to Makoto Demura; Faculty of Advanced Life Science, Hokkaido University, Sapporo 060-0810, Japan.

Phone & Fax: +81-11-706-2771, E-mail: demura@sci.hokudai.ac.jp

Highlights

- GR solubilized with DDM shows the pH-dependent trimer/monomer transition.
- His87-Asp121 salt bridge contributes to the trimer formation.
- His87 itself is essential for the trimer formation.
- The quaternary structure of GR may change during the photoreaction.
- The sign of bipolar CD spectra is opposite to those of BR and HR.

Abstract

Gloeobacter rhodopsin (GR) is a eubacterial proton pump having a highly conserved histidine near the retinal Schiff base counter-ion, aspartate. Various interactions between His and Asp of the eubacterial proton pump have been reported. Here, we showed the pH-dependent trimer/monomer transition of GR in the presence of dodecyl-β-D-maltoside by size-exclusion chromatography. The pH dependence was closely related to the protonation state of the counter-ion, Asp121. For the H87M mutant, pH dependence disappeared and a monomer became dominant. We concluded that the formation or breaking of the salt bridge between His87 and Asp121 inside the protein changes the quaternary structure.

Keywords

Microbial rhodopsin; Histidine-Aspartate cluster; Quaternary structure; Protonation; Size-exclusion chromatography; Circular dichroism spectroscopy

Abbreviations

GR, *Gloeobacter* rhodopsin; BR, bacteriorhodopsin; HR, halorhodopsin; SRII, sensory rhodopsin II; PR, proteorhodopsin; XR, xanthorhodopsin; ESR, *Exiguobacterium sibiricum* rhodopsin; DDM, dodecyl-β-D-maltoside; SEC, size-exclusion chromatography; PSB, protonated Schiff base; CD, circular dichroism; *E. coli*, *Escherichia coli*; *G. violaceus*, *Gloeobacter violaceus*; IPTG, isopropyl β-D-1-thiogalactopyranoside; MES, TES, TAPS, CHES, and CAPS, known abbreviations of Good's buffers.

1. Introduction

For light-driven proton-pumping rhodopsins recently discovered in eubacteria, the characteristic and unique histidine-aspartate (His-Asp) cluster is conserved, and its functional significance has been the subject of intensive studies [1-5]. Such a cluster is not present in archaeal proton-pumping rhodopsins such as the well-known bacteriorhodopsin (BR). Previous reports [2-5] have revealed that the His-Asp interaction contributes to the spectral tuning, partial protonation, and increased pK_a of the Asp residue as well as the primary photoreaction. The present study showed that this His-Asp interaction leads to the trimeric assembly of *Gloeobacter* rhodopsin (GR), and consequently the breaking of the salt bridge leads to the dissociation into monomers. This is an interesting observation in that the formation and breaking of the salt bridge inside the protein controls the protein's quaternary structure.

Recent advances in genomic technology have enabled the detection of the genes that encode retinal proteins in many microorganisms, and these proteins are referred to as microbial rhodopsins [6]. The world of microbial rhodopsins is expanding. From many eubacteria, light-driven proton-pumping rhodopsins have been discovered. Retinal binds to the lysine residue of the last and seventh helix via the protonated Schiff base (PSB), as is the case with BR. Illumination decreases the pK_a of PSB, and the proton of the Schiff base is transferred to the counter-ion (usually aspartate) of PSB. This is the first and key process of the photochemical function. Therefore, the aspartate as the counter-ion is highly conserved, as shown in Fig. 1-a, which also shows the conservation of this residue for archaeal rhodopsins except for halorhodopsin (HR), a light-driven Cl^- pump. In HR, the aspartate is replaced by the threonine residue to which Cl^- as a transport substrate binds. Moreover, for eubacterial proton-pumping rhodopsin, there is another highly conserved and characteristic histidine residue (see Fig. 1-a). The X-ray structure of xanthorhodopsin (XR) [1] revealed the formation of a cluster between these two residues (see Fig. 1-b and –c), and the functional significance of this cluster is a target of the investigation as described above.

2. Materials and methods

The detailed experimental procedures are described in Supplementary material.

2-1. Protein expression and purification

The histidine-tagged GR was expressed and purified according to a method used previously for *Natronomonas pharaonis* HR [7]. After purification, the sample media were replaced by the appropriate buffer solution by two passages over a PD-10 column (GE Healthcare UK, Amersham Place, England) for analysis.

2-2. Spectroscopy measurements

All the absorption spectra were recorded at 25^{o}C using a UV spectrophotometer (UV-1800, Shimadzu, Kyoto, Japan). Samples containing ca. 10 μM GR in 6-mix buffer (0.89 mM citrate, 0.89 mM MES, 1.1 mM TES, 0.78 mM TAPS, 1.1 mM CHES, 0.33 mM CAPS) with 0.3 M NaCl and 0.1% DDM were used.

For spectroscopic titration, the GR sample (ca. 10 μM) was first suspended in 6-mix buffer (pH ca. 10) containing 0.3 M NaCl and 0.1% DDM. Then the pH was adjusted to the desired value by the addition of a very small amount of 2 N H_2SO_4, followed by the measurement of absorption spectrum. The concentration change of GR was very small and was ignored.

The CD spectra of GR were measured by a Jasco J-725 spectropolarimeter (Jasco, Tokyo, Japan) in the 300-700 nm region at 25°C. The sample condition was the same as described above.

2-3. Size-exclusion chromatography (SEC)

Samples containing ca. 10 μM GR in the 6-mix buffer with 0.3 M NaCl and 0.1% DDM were applied to a Superdex 200 10/300 GL size-exclusion column (GE Healthcare UK, Amersham Place, England) equilibrated previously with the same buffer. The pH was adjusted to the desired value. All SEC experiments were performed at room temperature. The proteins were detected by the absorption of near the absorption maxima at each pH: for GR-WT, 550 nm at pH 2 and 3, 540 nm from pH 5 to 9; for GR-D121N, 550 nm at pH 2, 560 nm from pH 3 to 7.5, 570 nm at pH 9; for

GR-H87M, 560 nm at pH 2 and 3, 540 nm at pH 4, 520 nm from pH 5 to 9The molecular size was estimated by the standard method.

2-4. Analysis of SEC data

The SEC peak area was fitted by the sum of the Gram-Charlier peak function [8] (GCAS) using Origin Pro 8.6 J software (Origin Lab, Northampton, MA, USA). The peak areas of peak A (monomer), B (trimer), and C (oligomer) were calculated. According to the Henderson-Hasselbelch equation, the pK_a value of the monomer/trimer transition was estimated from the pH, giving half of the transition.

2-5. Assignment of SEC peaks

To estimate the amounts of DDM surrounding GR, we built the monomeric and trimeric model of GR using the crystal structure of XR [1] (PDB ID: 3DDL), which shares a high sequential homology with GR (ca. 70%). For the estimation of the trimeric form of GR, XR monomers were arranged according to the structure of BR trimer [9] (PDB ID: 1BRR). No further structural refinement was applied. According to references [10] and [11], the hydrophobic surface areas of the monomer and trimer were calculated to be 39.8 nm^2 and 119.4 nm^2, respectively, from which the masses of DDM binding were calculated. For peak C, the amounts of DDM adhering were not estimated because no structural information was known. The higher oligomer in peak C is supposed to be composed of *n* units of trimer because the CD spectrum of the peak C showed a single biphasic curve, the same as in the case of the trimeric peak B.

3. Results and Discussion

To determine the new function of the cluster, we focused on the oligomeric structure of GR. GR was found in the genome sequence of a thylakoidless unicellular cyanobacterium, *Gloeobacter violaceus* PCC 7421 [12]. For GR, the counter-ion is Asp121 [13,14] and the histidine is located at the 87th position (see Fig. 1-a). Figure 2-a shows the results for the wild-type GR (GR-WT) at pH 7.5 analyzed by size-exclusion chromatography (SEC). GR was expressed in *E. coli* membrane. Three peaks (labeled A, B, and C) are observed, showing the co-existence of three structural isomers. The affinity for the formation of the trimer structure is not so large that all molecules do not form the trimer in this condition. To assign these peaks, we compared SEC data on halorhodopsin from *Natronomonas pharaonis* (NpHR). Previously we showed that NpHR in the presence of DDM formed a trimer [10]. The dotted line in Fig. 2-a shows the chromatogram of the NpHR trimer, suggesting that peak B is attributable to the trimer. The F150W of NpHR forms a monomer in DDM solution [15], whose chromatogram is shown by the broken line in Fig. 2-a. This suggests that peak A is attributable to the monomer, although the difference in the elution volumes between peaks A and B is much larger than that of NpHR. This might be attributable to the difference in the masses of DDM surrounding the protein between NpHR and GR. Then, we calculated the masses of DDM adhering to the protein [10,11], which are listed in the right-most column of Table 1. For this calculation we used the structure of XR [1], since the similarity between XR and GR is high (~70%). From the observed elution volumes, the masses of the GR-DDM complex were calculated, and then the masses of GR were subtracted from those of the GR-DDM complex to estimate the masses of DDM adhering to GR (the second column from the right in Table 1). These values agree well with the theoretically calculated values. Therefore, we assigned peaks A, B, and C as a monomer, a trimer, and an oligomer, respectively. To confirm these, we measured CD spectra of each fraction (Fig. 2-b). The bipolar CD spectrum is the evidence of the trimer. Thus, panel b reveals the correct assignment of each fraction. It is noteworthy that the sign of the bipolar CD spectrum is opposite to that of BR [16] and HR [10,15,17,18]. The CD spectrum of GR exhibited a pair of negative and positive bands near 500 nm and 570 nm, respectively, and a zero crossover point near the absorption

maximum of 540 nm. The signals of the trimer and the oligomer are almost the similar. This suggests that the oligomer is an aggregation of the trimmers.

We performed the SEC experiments in varying pH, and the results are shown in Fig. 2-c, showing that the quaternary structure is pH dependent. In panel d, the relative contents of the monomer, trimer, and oligomer are plotted against pH. The ratio of the trimer increases as pH increases. Above pH 7.5, the trimer contents decrease and correspondingly that of the oligomer increases. Apart from this alkaline pH region, the pH dependence of the trimer and monomer ratios looks like a curve of the Henderson-Hasselbalch equation with a single pK_a value. A pK_a of ca. 4.8 was estimated, and we assumed that this pK_a is that of the counter-ion, Asp121. We then did the pH spectroscopic titration to estimate the pK_a of Asp121, since the protonation of the counter-ion shows the red-shift of the absorption maximum. The results are shown in Fig. 3, and pK_a was estimated to be ca. 4.5 which is close to 4.8. The blue shift at pH < 4 may be caused by the protonation of another residue. To confirm that the protonation state of Asp121 controls the trimer-monomer transition, we performed the SEC for the D121N mutant. The results shown in Fig. 4 indicate that the pH dependence of the trimer/monomer contents decreases. Thus, we conclude that the negative charge of Asp121 favors trimer formation. Figure 4 shows that the low pH-dependence of the D121N mutant remains, which might come from the dissociation/association states of some dissociable residues other than Asp121. This result suggests that the protonation state of Asp121 is a main factor, but some other residues also contribute to the trimer/monomer transition.

As described above, Asp121 is considered to form a cluster with His87, and then we examined the H87M mutant. Since the corresponding residue of BR is methionine, we prepared this mutant. The results of SEC analysis are shown in Fig. 4, indicating that the pH dependence of the trimer/monomer transition almost disappears, and that monomer is dominant. As described above, when Asp121 is protonated, the monomer is dominant (see Fig. 2-d). Then we might assume that in this H87M mutant, pK_a of Asp121 would increase significantly and this residue would be protonated in the pH range examined. We can rule out this possibility because of the pH dependence of the

absorption maxima of H87M (see below). Thus, we conclude that His87 is a key residue for trimer formation. If His87 does not exist, the deprotonation of carboxyls (mainly Asp121) and the protonation of amine do not lead to trimer formation.

The absorption maxima of the wild type, D121N, and H87M are shown in Fig. 3 as a function of pH. The reason for the red shift in the alkaline pH for all three proteins is not known at present. We can observe that there is essentially no pH dependence of the absorption maximum of D121N, revealing that the shift below pH 6 of the wild type and H87M is caused by the protonation of Asp121. It is noted that the wavelength changes of H87M are much larger than those of the wild type. Generally, pK_a of histidine is ca. 7, and then His87 in the wild type might be a neutral form at pH >7. If so, the maximum wavelength of the wild type at alkaline pH should be much closer to that of H87M. This suggests that even under alkaline conditions this histidine may be protonated. In fact, the pK_a of the corresponding histidine of a similar rhodopsin, ESR from *Exiguobacterium sibiricum*, is reported to be ca. 9 [5]. Above pH ca. 4.5 the counter-ion Asp121 is negatively charged (deprotonated), and the His87 may be positively charged to form an electrically stable cluster. Therefore, we conclude that the salt bridge between Asp121 in helix C and His87 in helix B is the main factor for trimer formation (see Fig. 1-b). Because of the salt bridge, the distance between helix B and helix C of XR, and possibly that of GR, is shorter than that of BR.

BR and HR also form a trimer, and the formation was attributed to the interaction of some specific residues with lipids [9,19,20] and to the interaction of some residues belonging to different molecules at the contact points [15,21,22]. On the other hand, the key residue of the trimer formation, His87, is located inside the protein (see Fig. 1-b and c) and not in the contact point. Therefore, molecular origin of the trimer formation of GR is different from those. The bipolar CD spectrum of the trimer of GR was observed (see Fig. 2-b, Fig. 5 in ref. [23], and Fig. 4A in ref. [24]), but the sign of the spectrum was opposite from BR [16] and HR [10,15,17,18]. One of possibility is that the molecular arrangement of the trimer structure of GR is different from that of BR and HR, but the further studies are awaited and in progress in our laboratory.

In BR and SRII (sensory rhodopsin II), the outward tilting of helix F during the photochemical cycle is confirmed [25-30]. This is considered to require the breaking of the salt bridge between the counter-ion in helix C and the PSB in helix G as one of the key steps. For SRII, some mutations breaking the salt bridges by substitutions of the counter-ions constitutively activate transducers even in the dark, while the extents depend on the replaced residues [28,31] Thus, the breaking of the salt bridge between two different helices could cause a conformational change. Of this notion, theobservation in the present paper is the similar as the helix tilting of BR and SRII. However, our observation is the much larger change of the trimer/monomer transition. The breaking of one salt bridge inside the protein induces the large change of the quaternary structure.

We observed the bipolar CD spectra also for *E. coli* cell membranes expressing GR, the sign of which was the same as that of DDM-solubilized GR (see Fig. 5). We may then consider that in the native cells GR forms the trimer, although in native cells, a carotenoid, echinenone, may bind to helix F of GR [24]. What is the physiological significance of the trimer formation? Although we don't yet know, we have the following observations. The H87M mutant (monomer) seems less stable in comparison to the wild type (trimer). Even for stable BR, the monomer is reported to be less stable under illumination than the wild trimer [32]. According to our preliminary data, the proton-pumping activity of the His mutant is ca. 50% that of the wild. Upon illumination, Asp121 receives the proton from PSB, thereby breaking the salt bridge. Therefore, in daylight, the monomer content increases whereas at night GR forms the trimer. We might imagine that this transition serves to transmit some information to the cytoplasm of native cells of *G. violaceus*, in addition to the proton pumping As shown in Fig. 1-a, the His-Asp cluster is highly conserved in light-driven proton-pumping proteins from eubacteria. The question then is whether or not all these proteins form a trimer. At least under certain conditions, PR forms the trimer (data not shown).

Acknowledgements

We thank T. Aizawa, M. Kamiya, and K. Kawano for their valuable comments.

References

[1] Luecke H, Schobert B, Stagno J, Imasheva ES, Wang JM, Balashov SP & Lanyi JK (2008) Crystallographic structure of xanthorhodopsin, the light-driven proton pump with a dual chromophore. *Proc Natl Acad Sci USA* **105**, 16561–16565.

[2] Rangarajan R, Galan JF, Whited G & Birge RR (2007) Mechanism of Spectral Tuning in Green-Absorbing Proteorhodopsin. *Biochemistry* **46**, 12679–12686.

[3] Bergo VB, Sineshchekov OA, Kralj JM, Partha R, Spudich EN, Rothschild KJ & Spudich JL (2009) His-75 in Proteorhodopsin, a Novel Component in Light-driven Proton Translocation by Primary Pumps. *J Biol Chem* **284**, 2836–2843.

[4] Hempelmann F, Hölper S, Verhoefen M-K, Woerner AC, Köhler T, Fiedler S-A, Pfleger N, Wachtveitl J & Glaubitz C (2011) His75-Asp97 Vluster in Green Proteorhodopsin. *J Am Chem Soc* **133**, 4645–4654.

[5] Balashov SP, Petrovskaya LE, Lukashev EP, Imasheva ES, Dioumaev AK, Wang JM, Sychev SV, Dolgikh DA, Rubin AB, Kirpichnikov MP & Lanyi JK (2012) Aspartate-Histidine Interaction in the Retinal Schiff Base Counterion of the Light-Driven Proton Pump of *Exiguobacterium sibiricum*. *Biochemistry* **51**, 5748–5762.

[6] Spudich, J. L.; Jung, K.-H. (2005) Microbial rhodopsin: Phylogenetic and functional diversity. In *Handbook of photosensory receptors* (Briggs, W. R., and Spudich, J. L., Eds.), pp 1-23, Wiley-VCH Verlag, Weinheim, Germany.

[7] Sato M, Kanamori T, Kamo N, Demura M & Nitta K (2002) Stopped-Flow Analysis on Anion Binding to Blue-Form Halorhodopsin from *Natronobacterium pharaonis*: Comparison with the Anion-Uptake Process during the Photocycle. *Biochemistry* **41**, 2452–2458.

[8] Di Marco VB & Bombi GG (2001) Mathematical functions for the representation of chromatographic peaks. *J Chromatogr A* **931**, 1–30.

[9] Essen L, Siegert R, Lehmann WD & Oesterhelt D (1998) Lipid patches in membrane protein oligomers: Crystal structure of the bacteriorhodopsin-lipid complex. *Proc Natl Acad Sci USA* **95**, 11673–11678.

[10] Sasaki T, Kubo M, Kikukawa T, Kamiya M, Aizawa T, Kawano K, Kamo N & Demura M (2009) Halorhodopsin from *Natronomonas pharaonis* Forms a Trimer Even in the Presence of a Detergent, Dodecyl-β-D-maltoside. *Photochem Photobiol* **85**, 130–136.

[11] Møller JV & le Maire M (1993) Detergent Binding as a Measure of Hydrophobic Surface Area of Integral Membrane Proteins. *J Biol Chem* **268**, 18659–18672.

[12] Nakamura Y, Kaneko T, Sato S, Mimuro M, Miyashita H, Tsuchiya T, Sasamoto S, Watanabe A, Kawashima K, Kishida Y, Kiyokawa C, Kohara M, Matsumoto M, Matsuno A, Nakazaki N, Shimpo S, Takeuchi C, Yamada M & Tabata S (2003) Complete Genome Structure of *Gloeobacter violaceus* PCC 7421, a Cyanobacterium that Lacks Thylakoids. *DNA Res* **10**, 137–145.

[13] Miranda MRM, Choi AR, Shi L, Bezerra AG Jr, Jung K-H & Brown LS (2009) The Photocycle and Proton Translocation Pathway in a Cyanobacterial Ion-Pumping Rhodopsin. *Biophys J* **96**, 1471–1481.

[14] Hashimoto K, Choi AR, Furutani Y, Jung K-H & Kandori H (2010) Low-Temperature FTIR Study of *Gloeobacter Rhodopsin*: Presence of Strongly Hydrogen-Bonded Water and Long-Range Structural Protein Perturbation upon Retinal Photoisomerization. *Biochemistry* **49**, 3343–3350.

[15] Tsukamoto T, Sasaki T, Fujimoto KJ, Kikukawa T, Kamiya M, Aizawa T, Kawano K, Kamo N & Demura M (2012) Homotrimer Formation and Dissociation of pharaonis Halorhodopsin in Detergent System. *Biophys J* **102**, 2906–2915.

[16] Heyn MP, Bauer PJ & Dencher NA (1975) A natural CD label to probe the structure of the purple membrane from *Halobacterium halobium* by means of exciton coupling effects. *Biochem Biophys Res Commun* **67**, 897–903.

[17] Hasselbacher CA, Spudich JL & Dewey TG (1988) Circular Dichroism of Halorhodopsin: Comparison with Bacteriorhodopsin and Sensory Rhodopsin I. *Biochemistry* **27**, 2540–2546.

[18] Yamashita Y, Kikukawa T, Tsukamoto T, Kamiya M, Aizawa T, Kawano K, Miyauchi S, Kamo N & Demura M (2011) Expression of *salinarum* halorhodopsin

in *Escherichia coli* cells: Solubilization in the presence of retinal yields the natural state. *Biochim Biophys Acta* **1808**, 2905–2912.

[19] Weik M, Patzelt H, Zaccai G & Oesterhelt D (1998) Localization of Glycolipids in Membranes by In Vivo Labeling and Neutron Diffraction. *Mol Cell* **1**, 411–419.

[20] Krebs MP & Isenbarger TA (2000) Structural determinants of purple membrane assembly. *Biochim Biophys Acta* **1460**, 15–26.

[21] Kolbe M, Besir H, Essen LO & Oesterhelt D (2000) Structure of the Light-Driven Chloride Pump Halorhodopsin at 1.8 A Resolution. *Science* **288**, 1390–1396.

[22] Kouyama T, Kanada S, Takeguchi Y, Narusawa A, Murakami M & Ihara K (2010) Crystal Structure of the Light-Driven Chloride Pump Halorhodopsin from *Natronomonas pharaonis*. *J Mol Biol* **396**, 564–579.

[23] Imasheva ES, Balashov SP, Choi AR, Jung K-H & Lanyi JK (2009) Reconstitution of *Gloeobacter violaceus* Rhodopsin with a Light-Harvesting Carotenoid Antenna. *Biochemistry* **48**, 10948–10955.

[24] Balashov SP, Imasheva ES, Choi AR, Jung K-H, Liaaen-Jensen S & Lanyi JK (2010) Reconstitution of Gloeobacter Rhodopsin with Echinenone: Role of the 4-Keto Group. *Biochemistry* **49**, 9792–9799.

[25] Kamikubo H, Kataoka M, Váró G, Oka T, Tokunaga F, Needleman R & Lanyi JK (1996) Structure of the N intermediate of bacteriorhodopsin revealed by x-ray diffraction. *Proc Natl Acad Sci USA* **93**, 1386–1390.

[26] Sass HJ, Büldt G, Gessenich R, Hehn D, Neff D, Schlesinger R, Berendzen J & Ormos P (2000) Structural alterations for proton translocation in the M state of wild-type bacteriorhodopsin. *Nature* **406**, 649–653.

[27] Subramaniam S & Henderson R (2000) Molecular mechanism of vectorial proton translocation by bacteriorhodopsin. *Nature* **406**, 653–657.

[28] Spudich EN, Zhang W, Alam M & Spudich JL (1997) Constitutive signaling by the phototaxis receptor sensory rhodopsin II from disruption of its protonated Schiff base-Asp-73 interhelical salt bridge. *Proc Natl Acad Sci USA* **94**, 4960–4965.

[29] Spudich JL (1998) Variations on a molecular switch: transport and sensory signalling by archaeal rhodopsins. *Mol. Microbiol.* **28**, 1051–1058.

[30] Wegener AA, Klare JP, Engelhard M & Steinhoff HJ (2001) Structural insights into the early steps of receptor-transducer signal transfer in archaeal phototaxis. *EMBO J.* **20**, 5312–5319.

[31] Sasaki J & Spudich JL (2008) Signal Transfer in Haloarchaeal Sensory Rhodopsin-Transducer Complexes. *Photochem Photobiol.* **84**, 863–868.

[32] Mukai Y, Kamo N & Mitaku S (1999) Light-induced denaturation of bacteriorhodopsin solubilized by octyl-β-glucoside. *Protein Eng.* **12**, 755–759.

Figure legends

Figure 1. (a) Amino acid sequence alignment of the His-Asp cluster region in eubacterial proton-pumping rhodopsins. GR, XR, PR, and ESR stand for *Gloeobacter* rhodopsin, xanthorhodopsin, proteorhodopsin, and *Exiguobacterium sibiricum* rhodopsin. This alignment also contains the corresponding sequences of archaeal rhodopsins. HsBR (bacteriorhodopsin, BR from *Halobacterium salinarum*), HsHR (halorhodopsin, HR from *H. salinarum*), and NpHR (HR from *Natronomonas pharaonis*) are light-driven ion pumps. Conserved aspartate and histidine residues are highlighted. Note that aspartate as the counter-ion of the protonate Schiff base is conserved for all except HR, while the histidine residue is conserved only in the eubacterial proton-pumping rhodopsins. (b) Top view of seven-helix XR from the cytoplasmic side using the X-ray crystal structure (PDB ID: 3DDL). Histidine in helix B, aspartate in helix C, and retinal (orange) are shown in the stick model. (c) Enlargement of the His-Asp cluster region, which is enclosed by the broken square in (b). The broken lines represent the supposed hydrogen bonds, and blue spherical dots represent water molecules.

Figure 2. SEC analysis of wild-type GR (GR-WT) in DDM solution (0.1%) at pH 7.5. The protein concentration was 10 μM in 0.3 M NaCl, and the temperature was 25^{o}C. (a) Three peaks, named A, B, and C, were assigned as a monomer, a trimer, and an oligomer. (b) CD spectra of the each fraction of A, B, and C, confirming the assignment. Dashed lines indicate the zero-base line. The scale bar represents the molar ellipticity of 10,000 [deg・cm^{2}・dml^{-1}]. (c) SEC chromatograms of GR-WT at various pH. (d) The percent ratios of monomer (black), trimer (red), and oligomer (blue) are plotted against pH.

Figure 3. The pH dependence of the absorption maxima of GR-WT (black circle), D121N (red square), and H87M (blue triangle). The protein concentration was 10 μM, which was dissolved in 0.3 M NaCl containing 0.1% DDM. The temperature was 25^{o}C.

Figure 4. (a) Size-exclusion chromatograms of GR-D121N (upper left) and GR-H87M (lower right) at various pH. (b) SEC analysis of D121N (square, solid line) and H87M (triangle, broken line). The ratios (peak area) are plotted against pH. Experimental conditions were the same as in Fig. 2.

Figure 5. CD spectra of the functionally-expressed GR in *E. coli* cell membrane (solid line) and DDM-solubilized GR (dashed line). The membrane sample was suspended in water (pH ca. 6) and then weakly sonicated to obtain a clear sample. The CD spectrum of the membrane sample in 300 - 450 nm region contained a contribution from the contamination by intrinsic *E. coli* cytochrome. The spectrum of the membrane sample exhibited a pair of negative and positive bands near 500 nm and 570 nm, respectively, and a zero crossover point near the absorption maximum of 540 nm, which are also observed in the DDM-solubilized GR.

Tables

Table 1. Calculated masses (kDa) of the GR-DDM complexes and DDM.

		SEC results			Theoretical
	Assembly	Complex	Protein	DDM	mass*
Peak A	Monomer	104.6	33.6	71.0	94.2
Peak B	Trimer	296.6	100.8	195.8	202.7
Peak C	Oligomer	621.9	-	-	-
NpHR-F150W	Monomer	136.2	32.4	103.7	96.4
NpHR-WT	Trimer	265.8	97.2	168.6	177.0

*DDM mass surrounding GR was estimated by reference to the previous methods [10, 11]. The DDM masses calculated from the SEC results agree with the theoretically calculated values.

Figures

Figure 1

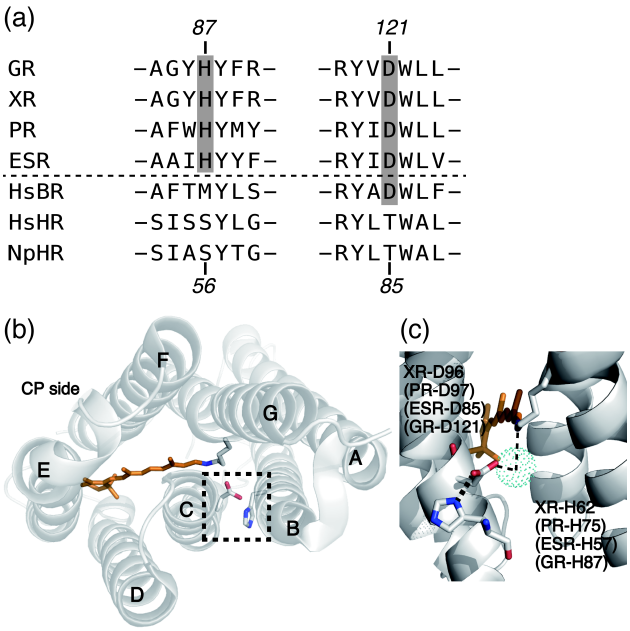

Figure 2

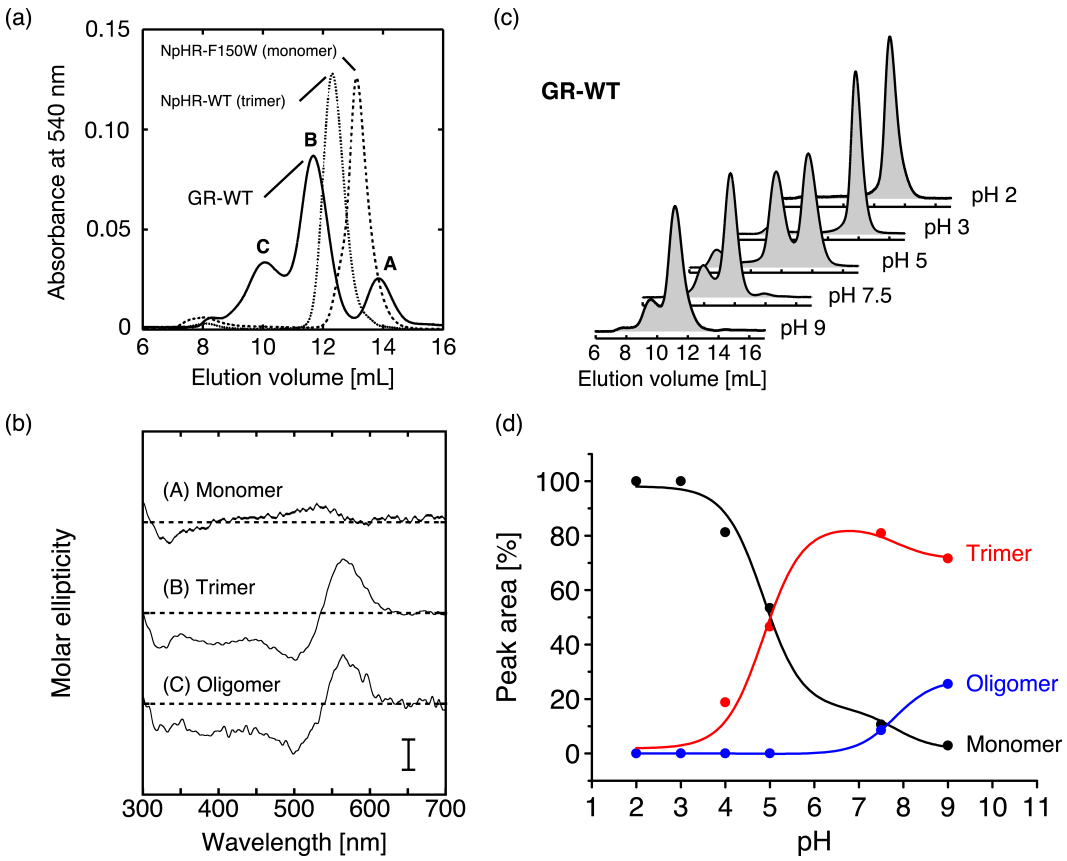
(a)
Absorbance at 540 nm
0.15
0.10
0.05
0
NpHR-F150W (monomer)
NpHR-WT (trimer)
GR-WT
A
B
C
6
8
10
12
14
16
Elution volume [mL]
(c)
GR-WT
pH 2
pH 3
pH 5
pH 7.5
pH 9
6 8 10 12 14 16
Elution volume [mL]
(b)
Molar ellipticity
(A) Monomer
(B) Trimer
(C) Oligomer
300
400
500
600
700
Wavelength [nm]
(d)
Peak area [%]
100
80
60
40
20
0
Trimer
Oligomer
Monomer
1 2 3 4 5 6 7 8 9 10 11
pH

Figure 3

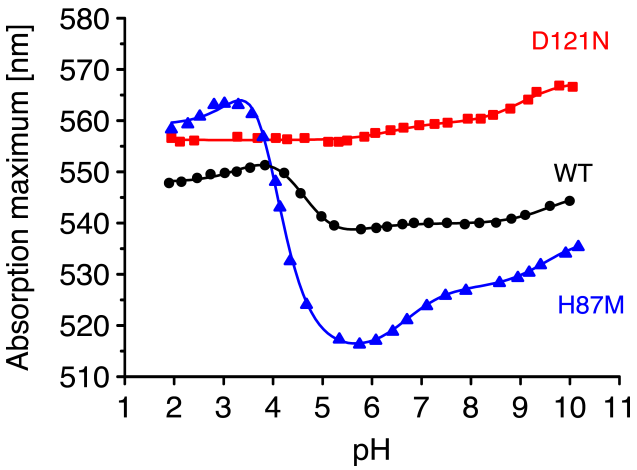
Absorption maximum [nm]
580
570
560
550
540
530
520
510
1
2
3
4
5
6
7
8
9
10
11
pH
D121N
WT
H87M

Figure 4

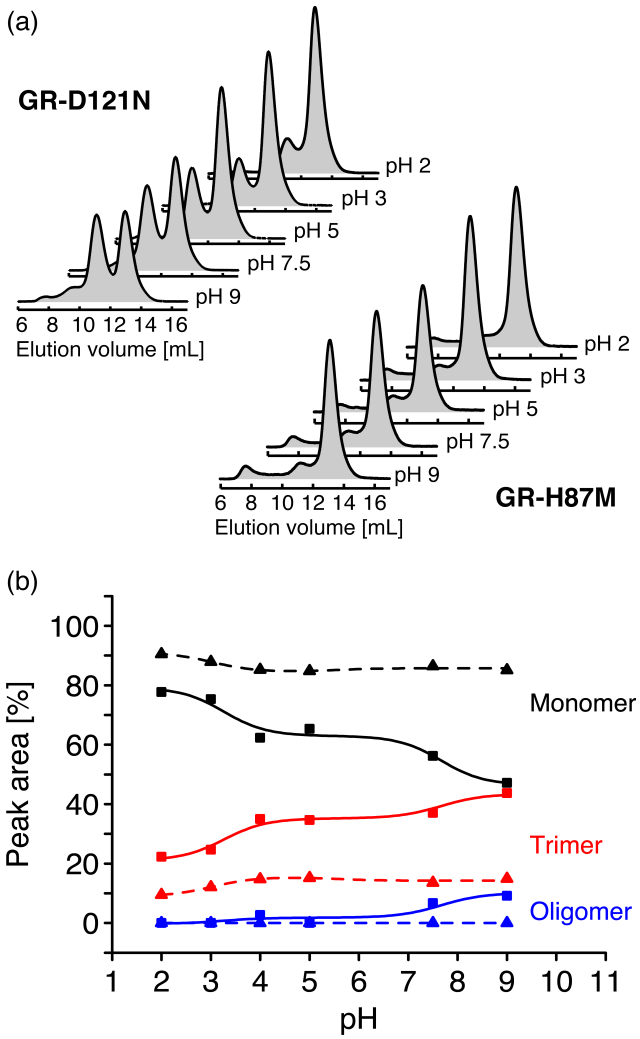
(a)
GR-D121N
pH 2
pH 3
pH 5
pH 7.5
pH 9
6 8 10 12 14 16
Elution volume [mL]
pH 2
pH 3
pH 5
pH 7.5
pH 9
GR-H87M
6 8 10 12 14 16
Elution volume [mL]
(b)
Peak area [%]
100
80
60
40
20
0
1 2 3 4 5 6 7 8 9 10 11
pH
Monomer
Trimer
Oligomer

Figure 5

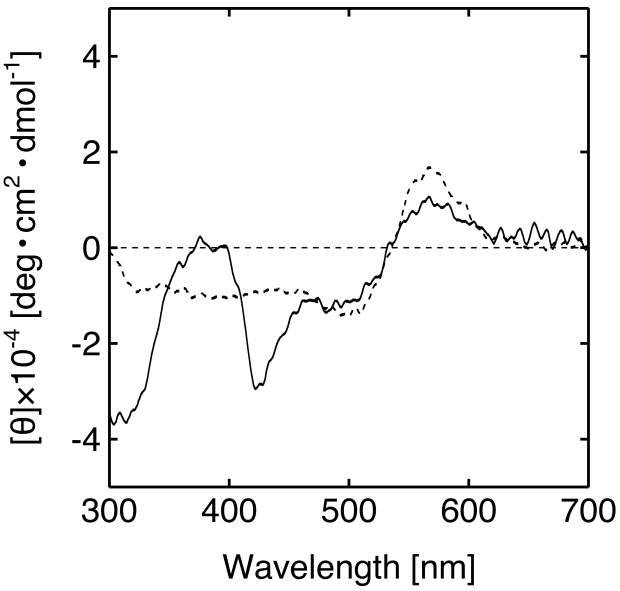

Supplementary material

Salt Bridge in the Conserved His-Asp Cluster in *Gloeobacter* Rhodopsin Contributes to Trimer Formation

Takashi Tsukamoto, Takashi Kikukawa, Takuro Kurata, Kwang-Hwan Jung, Naoki Kamo, and Makoto Demura

Experimental procedures

1. Recombinant DNA construction

A plasmid vector of wild-type GR with the additional C-terminal sequence LEHHHHHH was constructed by inserting the cloned genes into a pET-21c (+) (Novagen, Madison, WI, USA) expression vector. The plasmids of mutant GR were prepared using the Quikchange site-directed mutagenesis kit (Stratagene, La Jolla, CA, USA). The sense and anti-sense mutagenesis primers were: 5'-GAGTATCGCTGGGTACATGTACTTTCGGATCTTC-3' and 5'-GAAGATCCGAAAGTACATGTACCCAGCGATACTC-3' for GR-H87M; 5'-CGCCTACCGCTATGTGAACTGGCTGTTGACCGTGCC-3' and 5'-GGCACGGTCAACAGCCAGTTCACATAGCGGTAGGCG-3' for GR-D121N, respectively (Sigma-Aldrich, St. Louis, MO, USA). The correctness of the constructed plasmid DNA was confirmed by dideoxy sequencing (Applied Biosystems, Forster City, CA, USA).

2. Protein expression and purification

The histidine-tagged GR was expressed and purified according to a method used previously for *Natronomonas pharaonis* halorhodopsin [1]. Briefly, *E. coli* BL21(DE3) cells transformed by the expression plasmid were grown at 37^{o}C in 2 × YT medium containing 50 μg/mL ampicillin. After a 4-hour induction by 1 mM isopropyl β-D-1-thiogalactopyranoside (IPTG) with 10 μM all-trans retinal, colored cells were harvested by centrifugation (6400 × g for 10 min at 4^{o}C). The cells were suspended in 50 mM Tris-HCl buffer (pH 8) and disrupted by a French press (Ohtake, Tokyo, Japan)

(100 MPa × 4 times). The crude membrane fraction was collected by ultracentrifugation (178,000 × g for 90 min at 4°C). The collected fraction was solubilized with 1.5% n-dodecyl β-D-maltopyranoside (DDM) (Dojindo Lab, Kumamoto, Japan) in 50 mM Tris-HCl, pH 8, containing 0.3 M NaCl and 5 mM imidazole. After ultracentrifugation, the supernatant was incubated with Ni^{2+}-NTA agarose resin (Qiagen, Hilden, Germany). The resin was applied to a chromatography column and washed with 50 mM imidazole containing 50 mM Tris-HCl (pH 8), 0.3 M NaCl, and 0.1% DDM. The DDM-solubilized GR was collected by elution with the same buffer containing 0.3 M imidazole. The sample media were replaced by the appropriate buffer solution by two passages over a PD-10 column (GE Healthcare UK, Amersham Place, England).

3. Spectroscopy measurements

All the absorption spectra were recorded at 25°C using a UV spectrophotometer (UV-1800, Shimadzu, Kyoto, Japan). Samples containing ca. 10 μM GR in 6-mix buffer (0.89 mM citrate, 0.89 mM MES, 1.1 mM TES, 0.78 mM TAPS, 1.1 mM CHES, 0.33 mM CAPS) with 0.3 M NaCl and 0.1% DDM were used.

For spectroscopic titration, the GR sample (ca. 10 μM) was first suspended in 6-mix buffer (pH ca. 10) containing 0.3 M NaCl and 0.1% DDM. Then the pH was adjusted to the desired value by the addition of a very small amount of 2 N H_2SO_4, followed by the measurement of absorption spectrum. The concentration change of GR was very small and was ignored.

The CD spectra of GR were measured by a Jasco J-725 spectropolarimeter (Jasco, Tokyo, Japan) in the 300-700 nm region at 25°C at a scanning speed of 200 nm/min, and the accumulation was carried out four times. The sample condition was the same as described above. For the visible CD measurement of GR in *E. coli* cell membrane, the membrane was isolated by the standard method. To reduce scattering, the membrane was sonicated weakly and washed several times with water.

4. Size-exclusion chromatography (SEC)

Samples containing ca. 10 μM GR in the 6-mix buffer with 0.3 M NaCl and 0.1% DDM were applied to a Superdex 200 10/300 GL size-exclusion column (GE Healthcare UK, Amersham Place, England, total bed volume; V_t = 24 [mL])

equilibrated previously with the same buffer. The pH was adjusted to the desired value. All SEC experiments were performed at room temperature. The program was run at a flow rate of 0.4 mL/min, and the proteins were detected by the absorption of near the absorption maxima at each pH: for GR-WT, 550 nm at pH 2 and 3, 540 nm from pH 5 to 9; for GR-D121N, 550 nm at pH 2, 560 nm from pH 3 to 7.5, 570 nm at pH 9; for GR-H87M, 560 nm at pH 2 and 3, 540 nm at pH 4, 520 nm from pH 5 to 9 (BioLogic^{TM} DuoFlow, BioRad Laboratories, La Jolla, CA). The molecular size was estimated by the standard method.

5. Analysis of SEC data

The SEC peak area was fitted by the sum of the Gram-Charlier peak function [2] (GCAS) using Origin Pro 8.6 J software (Origin Lab, Northampton, MA, USA). The peak areas of peak A (monomer), B (trimer), and C (oligomer) were calculated. According to the Henderson-Hasselbelch equation, the pK_a value of the monomer/trimer transition was estimated from the pH, giving half of the transition.

6. Assignment of SEC peaks

To estimate the amounts of DDM surrounding GR, we built the monomeric and trimeric model of GR using the crystal structure of xanthorodopsin [3] (XR, PDB entry is 3DDL), which shares a high sequential homology with GR (ca. 70%). For the estimation of the trimeric form of GR, XR monomers were arranged according to the structure of bacteriorhodopsin (BR) trimer [4] (PDB entry is 1BRR). No further structural refinement was applied. According to references [5] and [6], the hydrophobic surface areas of the monomer and trimer were calculated to be 39.8 nm^2 and 119.4 nm^2, respectively, from which the masses of DDM binding were calculated. For peak C, the amounts of DDM adhering were not estimated because no structural information was known. The higher oligomer in peak C is supposed to be composed of *n* units of trimer because the CD spectrum of the peak C showed a single biphasic curve, the same as in the case of the trimeric peak B.

References

[1] Sato M, Kanamori T, Kamo N, Demura M & Nitta K (2002) Stopped-Flow Analysis on Anion Binding to Blue-Form Halorhodopsin from *Natronobacterium pharaonis*: Comparison with the Anion-Uptake Process during the Photocycle. *Biochemistry* **41**, 2452–2458.

[2] Di Marco VB & Bombi GG (2001) Mathematical functions for the representation of chromatographic peaks. *J Chromatogr A* **931**, 1–30.

[3] Luecke H, Schobert B, Stagno J, Imasheva ES, Wang JM, Balashov SP & Lanyi JK (2008) Crystallographic structure of xanthorhodopsin, the light-driven proton pump with a dual chromophore. *Proc Natl Acad Sci USA* **105**, 16561–16565.

[4] Essen L, Siegert R, Lehmann WD & Oesterhelt D (1998) Lipid patches in membrane protein oligomers: crystal structure of the bacteriorhodopsin-lipid complex. *Proc Natl Acad Sci USA* **95**, 11673–11678.

[5] Sasaki T, Kubo M, Kikukawa T, Kamiya M, Aizawa T, Kawano K, Kamo N & Demura M (2009) Halorhodopsin from *Natronomonas pharaonis* Forms a Trimer Even in the Presence of a Detergent, Dodecyl-β-D-maltoside. *Photochem Photobiol* **85**, 130–136.

[6] Møller JV & le Maire M (1993) Detergent Binding as a Measure of Hydrophobic Surface Area of Integral Membrane Proteins. *J Biol Chem* **268**, 18659–18672.